

SPIN-CURRENT IN A MAGNETIC SEMICONDUCTOR TUNNEL JUNCTION: EFFECT OF EXTERNAL BIAS VOLTAGE

LOAN T. NGUYEN^{1,2}, H.-J. DROUHIN³ AND HOAI T. L. NGUYEN^{2,4†}

¹*Hong Duc University, 565 Quang Trung road, Dong Ve, Thanh Hoa, Vietnam*

²*Graduate University of Science and Technology, Vietnam Academy of Science and Technology (VAST), 18 Hoang Quoc Viet, Cau Giay, Hanoi, Vietnam*

³*Laboratoire des Solides Irradiés, École Polytechnique, CNRS, CEA/DRF/IRAMIS, Institut Polytechnique de Paris, 91128 Palaiseau cedex, France*

⁴*Institute of Physics, Vietnam Academy of Science and Technology (VAST), 10 Daotian, Badinh, Hanoi, Vietnam*

E-mail: [†]nlhoai@iop.vast.vn

Received 4 June 2022

Accepted for publication 8 July 2022

Published 6 September 2022

Abstract. *This paper investigates spin-current transport in GaMnAs/GaAs/GaMnAs magnetic semiconductor tunnel junctions under applied bias voltages. The 30-band $\mathbf{k}\cdot\mathbf{p}$ approach is used to describe the materials within the heterostructure, incorporating both spin-orbit and exchange interactions. We use the transfer-matrix formalism to derive numerical solutions for the wave functions. At specific bias values, we calculate the polarization of the spin-current component along the z direction of the structure. We show oscillations of the two spin-current components perpendicular to the magnetization with equal polarization amplitude and characteristic period. The polarization amplitude varies around 10%, reflecting the typical polarization in such type of material. The oscillation period - which relates to the Larmor frequency for spin precession - increases with the bias voltage values.*

Keywords: spin-orbit interaction, III-V semiconductor, magnetic tunnel junction, spin-current, multi-band transport, transfer matrix, $\mathbf{k}\cdot\mathbf{p}$ method.

Classification numbers: 85.75.-d; 75.76.+j; 71.15.Ap.

I. INTRODUCTION

Spintronics is an emerging research field that studies electron spin properties to improve the efficiency and design new functionalities of electronic devices. Therein, manipulating the device magnetization states is one of the main objectives which could be reached with the use of polarized spin currents [1, 2]. The spin currents pass through the structure, interact with it, and exert spin torques on the local magnetization. Part of the spin momentum is transferred to the local magnetization, resulting in a re-orientation or reversing its direction. This effect, the so-called current-induced magnetization switching (CIMS), has been experimentally found in various classes of materials, including metallic, topological insulators, and magnetic semiconductors [3–7]. It is nowadays spintronics core technology, providing prospects for engineering a new memory device generation with high speed and high information storage density [8].

A detailed analysis of spin currents is important to understand the switching mechanism [7]. Spin current is generally understood as the difference between the electron currents carrying up spins and down spins within the system. In term of quantum mechanics, the spin current can be calculated as the expectation value of the spin current operator - the dyadic product of the velocity and Pauli operators [9]: $\hat{\mathbf{j}}_s \sim \hat{\mathbf{v}} \otimes \hat{\boldsymbol{\sigma}}$. Here the velocity $\hat{\mathbf{v}}$ is defined from the Hamiltonian, $\hat{v}_j = \frac{\partial \hat{H}}{\partial p_j}$. This expression is valid in systems with Hamiltonians containing up to second-order terms in the momentum operator [10] and is so far considered as the canonical definition for spin currents. Nevertheless, the study of the spin-current profile remains quite limited and is only performed in effective models where the wave functions are relatively simple [11–14].

Magnetic Tunnel Junctions (MJTs) are essential structures for Magnetoresistive Random Access Memory (MRAM) applications [8]. Meanwhile, GaAs and GaMnAs, with the simultaneous presence of exchange and spin-orbit coupling, are promising platforms for novel spin-related effects [15]. It has been shown that CIMS may happen in GaMnAs-based MJTs without external magnetic field. The critical current density for switching is hundred of times less than that in traditional metal MTJs [3, 16]. However, studying spin transport in such systems is challenging as it involves the contribution of multi-electronic bands. In recent works, we have developed $\mathbf{k} \cdot \mathbf{p}$ codes up to forty bands with spurious state removal, which can perfectly describe the spin-related phenomena in III-V semiconductor systems [16, 17]. In this paper, we will use our 30-band $\mathbf{k} \cdot \mathbf{p}$ codes to investigate the concept of polarized spin current in a GaMnAs/GaAs/GaMnAs MJT structure in the case when an external bias voltage is applied. We will compute the profile of the three spin components along the structure z direction and then study the dependence of the spin-current properties on the bias values.

II. PROBLEM DESCRIPTION AND METHOD

II.1. Problem description

We consider the MTJ structure formed by a GaAs-based semiconductor heterojunction grown along the [001] crystal axis. This structure, shown in Fig. 1, consists of a layer of intrinsic GaAs semiconductor with thickness d_2 acting as a potential barrier, sandwiched between two GaMnAs layers on the left and right sides with thicknesses d_1 and d_3 respectively. The structure is in the spin-transfer configuration with the magnetization directions of the two GaMnAs layers perpendicular to each other. The energy difference between the two bandgaps of the GaAs and GaMnAs layers defines the barrier height V_b . The whole structure is placed under a forward

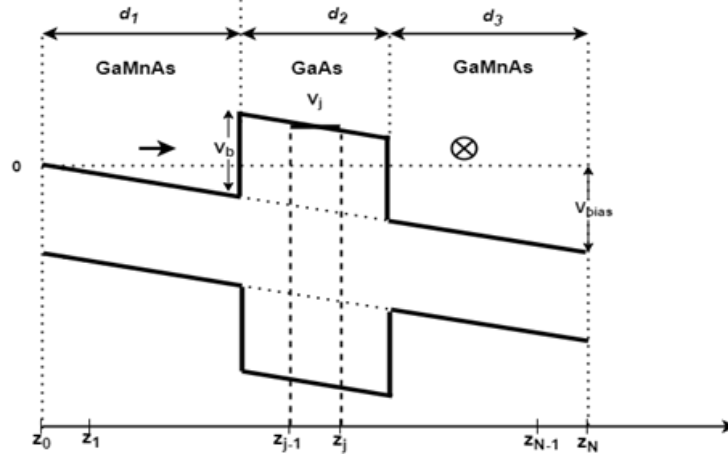


Fig. 1. Tunneling through a GaMnAs/GaAs/GaMnAs magnetic tunnel junction with spin-transfer configuration under applied bias voltage.

electrical bias voltage $U_{bias} > 0$. A particle of energy E_f is injected obliquely into the system with the in-plane wave vector components $[k_x, k_y]$. The Schrödinger equation for the wave function writes:

$$(\hat{H} + V) |\Psi\rangle = E |\Psi\rangle. \quad (1)$$

Here \hat{H} is the $\mathbf{k} \cdot \mathbf{p}$ Hamiltonian and $V = V_0 + V_{ext}(z)$ is the potential, where

$$V_0 = \begin{cases} V_b & \text{if } d_1 \leq z \leq d_1 + d_2, \\ 0 & \text{otherwise,} \end{cases} \quad (2)$$

and

$$V_{ext}(z) = -V_{bias} \frac{z}{d_1 + d_2 + d_3}. \quad (3)$$

describe the potential drop from the left to right electrode resulting of the applied bias voltage; here $V_{bias} = eU_{bias} > 0$.

II.2. Computation Method

To describe the energy structure of the semiconductor layers, we use the 30-band $\mathbf{k} \cdot \mathbf{p}$ formalism in which the Hamiltonian takes the form of a 30×30 matrix written in the basis functions of the $\{\Gamma_{6q}, \Gamma_{8d}, \Gamma_{7d}, \Gamma_{8-3}, \Gamma_{6u}, \Gamma_{8C}, \Gamma_{7C}, \Gamma_6, \Gamma_8, \Gamma_7, \Gamma_{6V}\}$ band set in the T_d group [18]. For the GaAs layer, we take the Hamiltonian expression in Ref. [18], with the parameters from Ref. [19]. For GaMnAs layers, an additional term describing the exchange interaction is taken into account, which generally has the form of a block-diagonal matrix:

$$\hat{H}_{exc} = \text{diag}(W_{exc}^{\Gamma_{6q}}, W_{exc}^{\Gamma_{7d,8d}}, W_{exc}^{\Gamma_{8-3}}, W_{exc}^{\Gamma_{6u}}, W_{exc}^{\Gamma_{7C,8C}}, W_{exc}^{\Gamma_6}, W_{exc}^{\Gamma_{7,8}}, W_{exc}^{\Gamma_{6V}}), \quad (4)$$

with

$$W_{exc}^{\Gamma_j} = \omega^{\Gamma_j} \mathbf{s}^{\Gamma_j} \cdot \mathbf{m}. \quad (5)$$

Here ω^{Γ_j} and \mathbf{s}^{Γ_j} are the exchange energy and spin vector in the subspace Γ_j , and \mathbf{m} is the unit vector along the magnetization direction. In this article we make the approximation that only

the exchange interaction acting on the first conduction Γ_6 and upper valence bands $\Gamma_{7,8}$ gives significant contribution. Expressions for the spin vectors \mathbf{s}^{Γ_6} and $\mathbf{s}^{\Gamma_{7,8}}$ have been derived in the Ref. [20].

We will reformulate the transfer matrix for solving the tunneling problem in the case of an arbitrary potential barrier [21] in a multi-band description. The structure in Fig. 1 is divided into N small barrier steps, separated by interfaces located at the coordinates $\{z_0, z_1, \dots, z_N\}$. The j th region within the interval $[z_{j-1}, z_j]$ is supposed to have a constant potential:

$$V_j = V_0 - \frac{j}{N} V_{bias}. \quad (6)$$

Near the interface at z_j , the wave function is of the form

$$\Psi^{j,L} = \sum_{m=1}^M a_m^{(j,L)} \Phi_m^{(j,L)}(k_m^{(j,L)}) \exp(ik_m^{(j,L)} z) + b_m^{(j,L)} \Phi_m^{(j,L)}(-k_m^{(j,L)}) \exp(-ik_m^{(j,L)} z) \quad (7)$$

at the left of the interface, and

$$\Psi^{j,R} = \sum_{m=1}^M a_m^{(j,R)} \Phi_m^{(j,R)}(k_m^{(j,R)}) \exp(ik_m^{(j,R)} z) + b_m^{(j,R)} \Phi_m^{(j,R)}(-k_m^{(j,R)}) \exp(-ik_m^{(j,R)} z) \quad (8)$$

at the right of the interface. In Eqs. (7)-(8), $M = 30$ is the number of electron bands; $k_m^{j,L(R)}$ is the wave vector, being solution of the equation:

$$\det \|(H_{\mathbf{k},\mathbf{p}}^{j,L(R)} + V^{j,L(R)} - E)\| = 0, \quad (9)$$

and $\Phi_m^{j,L(R)}$ is the corresponding eigenvector. Note that Eq. (9) has $2M$ solutions in general. According to time inversion, if k_m^j is a solution then $-k_m^j$ is also a solution, so that in Eqs. (7)-(8), we have arranged $-k_m^j \equiv k_{m+M}^j$; the sum is therefore taken over $m \in \{1 \dots M\}$. It is worth noting that $V_j^{j,L} = V_j$ while $V_j^{j,R} = V_{j+1}$. By convention, we denote $A^j = [a_1^{(j)}, a_2^{(j)}, \dots, a_M^{(j)}]^T$ and $B^j = [b_1^{(j)}, b_2^{(j)}, \dots, b_M^{(j)}]^T$. Remembering that the current density operator is $\hat{J}_j = \partial \hat{H} / \partial p_j$, the boundary conditions that Ψ and $J_z \Psi$ are continuous at each interface $z = z_j$, ($j = 0 \dots N$) yield

$$M^{j,L} \begin{bmatrix} A^{j,L} \\ B^{j,L} \end{bmatrix} = M^{j,R} \begin{bmatrix} A^{j,R} \\ B^{j,R} \end{bmatrix}, \quad (10)$$

where $M^{j,L(R)}$ are $2M \times 2M$ matrices constructed from the $\Phi_m^{j,L(R)}$ eigenvectors and from the action of the current operator on the plane-wave part of the wave function

$$M^{j,L(R)} = \begin{bmatrix} [\Phi_1^{j,L(R)}] & \dots & [\Phi_{2M}^{j,L(R)}] \\ [(J_z \exp ik_1^{j,L(R)} z|_{z=0}) \Phi_1^{j,L(R)}] & \dots & [(J_z \exp ik_{2M}^{j,L(R)} z|_{z=0}) \Phi_{2M}^{j,L(R)}] \end{bmatrix}. \quad (11)$$

Also note that $\begin{bmatrix} A^{j-1,R} \\ B^{j-1,R} \end{bmatrix}$ and $\begin{bmatrix} A^{j,L} \\ B^{j,L} \end{bmatrix}$ are related by

$$\begin{bmatrix} A^{j,L} \\ B^{j,L} \end{bmatrix} = Q^j \begin{bmatrix} A^{j-1,R} \\ B^{j-1,R} \end{bmatrix}, \quad (12)$$

where Q^j is a diagonal matrix

$$Q^j = \begin{pmatrix} \exp(ik_1^j d^j) & \dots & \dots & 0 \\ \dots & \dots & \dots & \dots \\ \dots & \dots & \dots & \dots \\ 0 & \dots & \dots & \exp(ik_{2M}^j d^j) \end{pmatrix}. \quad (13)$$

We obtain

$$\begin{pmatrix} A^{N,R} \\ B^{N,R} \end{pmatrix} = [M^{N,R}]^{-1} [M^{N,L}] [Q^N] [M^{N-1,R}]^{-1} [M^{N-1,L}] [Q^{N-1}] \dots \\ \dots [M^{1,R}]^{-1} [M^{1,L}] [Q^1] [M^{0,R}]^{-1} [M^{0,L}] \begin{pmatrix} A^{0,L} \\ B^{0,L} \end{pmatrix}. \quad (14)$$

In the case where the electrodes before the first layer on the left and after the last layer on the right have the same configuration, we have

$$[M^{N,R}] = [M^{0,L}] = M^e, \quad (15)$$

and

$$\begin{pmatrix} A^{N,R} \\ B^{N,R} \end{pmatrix} = \prod_{i=N}^1 T_i \begin{pmatrix} A^{0,L} \\ B^{0,L} \end{pmatrix}. \quad (16)$$

We thus recover the usual formula

$$\begin{pmatrix} A^R \\ B^R \end{pmatrix} = T \begin{pmatrix} A^L \\ B^L \end{pmatrix}, \quad (17)$$

with $T = \prod_{i=N}^1 T_i$ being the transfer matrix of the whole structure calculated by taking the product of the transfer matrices representing the constitutive barriers $T_i = [M^e]^{-1} [M^{i,L}] Q^i [M^{i-1,R}]^{-1} [M^e]$.

III. RESULTS AND DISCUSSION

We consider here a MJT structure made of GaMnAs (20 nm)/ GaAs (5 nm)/GaMnAs (40 nm) under the presence of external bias voltages. Note that in the actual devices, the right electrode (the so-called free electrode) is made very thin so that the magnetization switching could happen easily. However, in this paper, we have modelled a thick one in order to investigate the entire properties of spin current over space. The magnetization of the left GaMnAs layer is parallel to the z direction, while that of the right GaMnAs layer is along the x direction (Fig. 1). Conduction-band electrons are injected into the structure at a kinetic energy $E_f = 0.16$ eV counted from the bottom of the conduction band with the in-plane wave-vector components $[k_x, k_y] = [0.01, 0.01] \text{ \AA}^{-1}$. The barrier height is chosen as $V_b = 0.3$ eV. The exchange energy is $\omega = 0.05$ eV in both GaMnAs electrodes.

The spurious states are removed with the use of an advanced ghost-band technique [16]. Then, the tunneling problem is solved using the transfer matrix method described in Section II: electron transmission and wavefunctions in the space are derived. Figure 2 shows the calculation result for electron transmission, which non-linearly increases with the bias voltage. The transmission curve is symmetric for reverse bias voltages ($U_{bias} < 0$) and its value decreases with the barrier

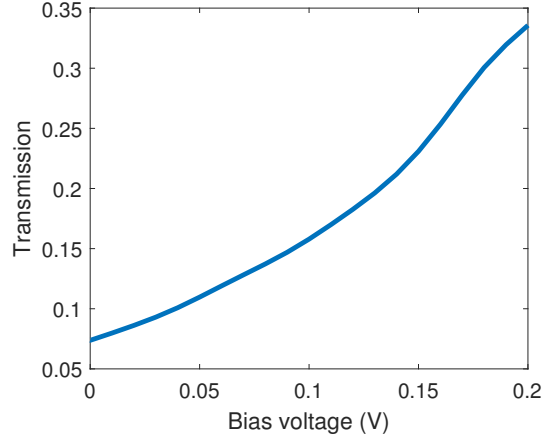


Fig. 2. Electron transmission vs. applied bias voltage.

thickness. Once the wave function is obtained, we calculate the probability current $\langle \Psi | \hat{J}_i | \Psi \rangle$ and spin current $\langle \Psi | \hat{J}_i^\alpha | \Psi \rangle$, where \hat{J}_i^α is the spin-current operator [9, 10]:

$$\hat{J}_{i\alpha} = \frac{1}{2} (\hat{v}_i \hat{\sigma}_\alpha + \hat{\sigma}_\alpha \hat{v}_i). \quad (18)$$

Here, the subscripts $i = \{x, y, z\}$ represent space coordinates and $\alpha = \{\sigma_x, \sigma_y, \sigma_z\}$ are spin components. Along the z direction, we thus have three spin-current components $J_{z\sigma_x}$, $J_{z\sigma_y}$, and $J_{z\sigma_z}$. We introduce the ratios between the spin-current components and the probability current which have the meaning of spin-current polarizations:

$$P_{\sigma_x}(z) = \frac{\langle \Psi | \hat{J}_{z\sigma_x} | \Psi \rangle}{\langle \Psi | \hat{J}_z | \Psi \rangle}; \quad P_{\sigma_y}(z) = \frac{\langle \Psi | \hat{J}_{z\sigma_y} | \Psi \rangle}{\langle \Psi | \hat{J}_z | \Psi \rangle}; \quad P_{\sigma_z}(z) = \frac{\langle \Psi | \hat{J}_{z\sigma_z} | \Psi \rangle}{\langle \Psi | \hat{J}_z | \Psi \rangle}. \quad (19)$$

We have checked that the probability current is constant within the structure at a given bias voltage value. The spin-current polarizations in Eq. (19) are thus proportional to and behave in the same way as the spin-current components over the whole space.

Figure 3 presents the spin-current polarization P_{σ_x} (blue dotted line), P_{σ_y} (red dashed line), and P_{σ_z} (yellow solid line) along the structure z direction for several bias values: $U_{bias} = 0$ V (upper, left), $U_{bias} = 0.05$ V (upper, right), $U_{bias} = 0.1$ V (lower, left), and $U_{bias} = 0.15$ V (lower, right). The vertical axis represents the absolute value of the spin-current polarization using a logarithm scale and the horizontal axis represents the coordinate along the z direction. In all cases, we observe a similar behavior of the spin-current polarization compared to the case of a voltage-free structure [16, 22], i.e., $U_{bias} = 0$ V: the spin-current injected from the left GaMnAs electrode, strongly attenuated in the barrier from the left interface, then a little bit re-enhanced near the right interface, finally enters the right GaMnAs electrode with an amplitude depending on the bias voltage. It is worth noting that P_{σ_z} is nearly constant in the left electrode and that P_{σ_x} is nearly constant in the right electrode. For semiconductor conduction bands, we recover the same conclusion which was experimentally obtained [23] and theoretically proved [24] for magnetic metals that the spin-current component parallel to the magnetization plays no role in the spin-transfer-torque effect.

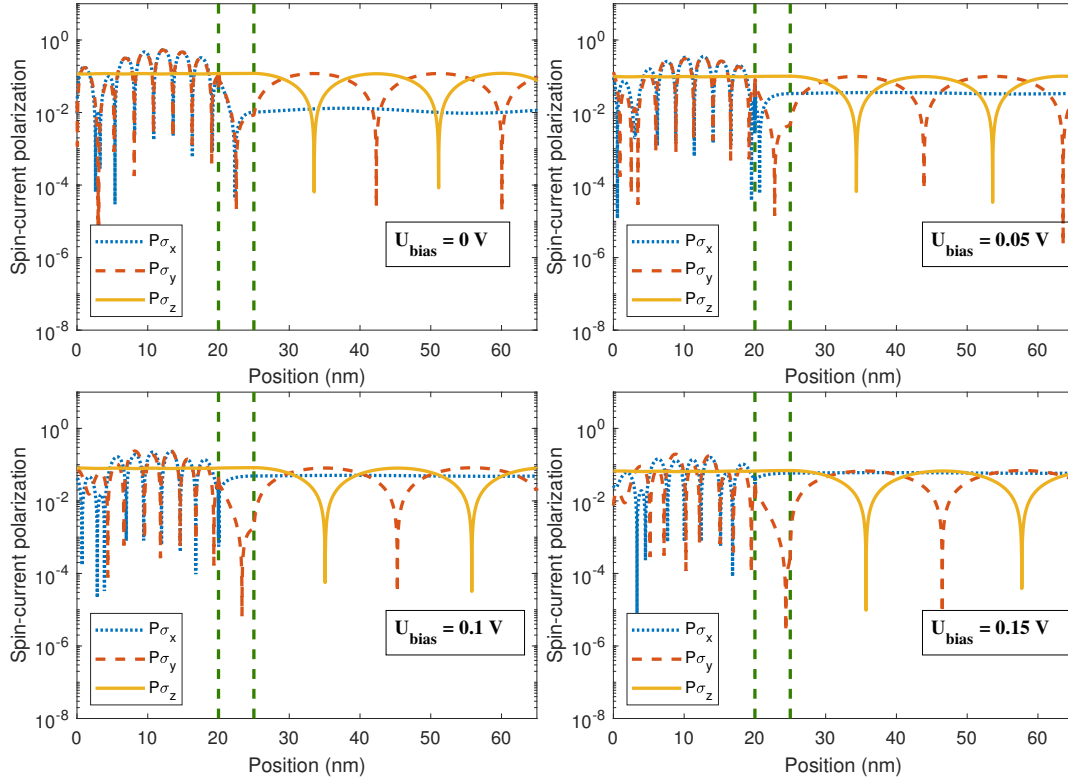


Fig. 3. Spin-current polarization P_{σ_x} (blue dotted line), P_{σ_y} (red dashed line), and P_{σ_z} (yellow solid line) along the structure z -direction for $U_{bias} = 0$ V (upper, left), $U_{bias} = 0.05$ V (upper, right), $U_{bias} = 0.1$ V (lower left), and $U_{bias} = 0.15$ V (lower, right).

In the right electrode, the two spin-current components P_{σ_y} and P_{σ_z} , which are perpendicular to the magnetization and thus responsible for the spin-transfer torques, oscillate along z with a characteristic period and polarization amplitude. They are just shifted from each other by a phase factor $\approx \pi/4$. The oscillation period can be determined by twice the distance between two adjacent minimum points on the relevant curves: $\lambda = 35.0$ nm for $U_{bias} = 0$ V, $\lambda = 38.6$ nm for $U_{bias} = 0.05$ V, $\lambda = 41.4$ nm for $U_{bias} = 0.1$ V, and $\lambda = 44$ nm for $U_{bias} = 0.15$ V. This length relates to the Larmor frequency describing spin precession and seems to increase with bias voltage. A detailed analysis of the P_{σ_x} , P_{σ_y} , and P_{σ_z} amplitudes in the right GaMnAs electrode is shown in Fig. 4. The results indicate that the values of the spin-current polarizations are less than 10%, which is the typical polarization in such type of materials [9]. The P_{σ_x} amplitude is small, of about 1% at $U_{bias} = 0$ V and increases as the bias voltage increases. The amplitudes of P_{σ_y} and P_{σ_z} are found to be equal for all bias voltages, being $\approx 11\%$ at $U_{bias} = 0$ V, and decrease to 6% at 0.2 V.

At a given location, P_{σ_y} and P_{σ_z} will contribute in proportion to the field-like torque and anti-damping torque which govern the local magnetization switching dynamics *via* the Landau-Lifshitz-Gilbert-Slonczewski (LLGS) equation [1]. It is important to see how they vary with the bias voltage. Fig. 5 shows their values calculated at the location $z = 35$ nm: while P_{σ_y} only slightly changes, P_{σ_z} undergoes a direction reversal at $U_{bias} \approx 0.1$ V. The Slonczewski torque, proportional

to $\partial P_{\sigma_z}/\partial z$ [10, 17], thus reaches a maximum, indicating that the local magnetization switching may occur in neighbourhood of this voltage value.

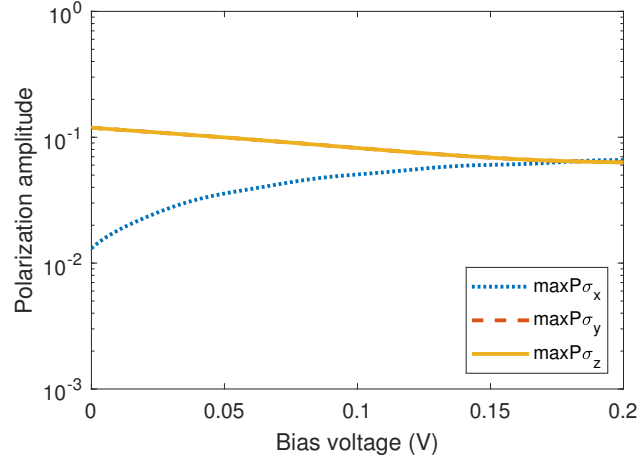


Fig. 4. Dependence of the spin-current polarization amplitudes on the bias voltage. The $\max P_{\sigma_y}$ (red) and $\max P_{\sigma_z}$ (yellow) lines overlap and show the equivalence of P_{σ_y} and P_{σ_z} amplitudes for all bias voltage values.

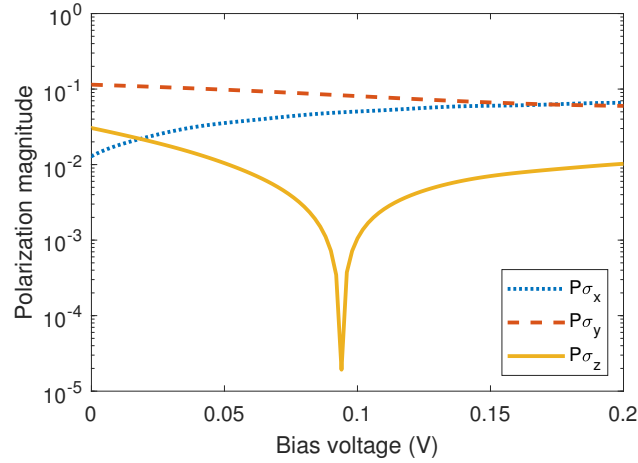


Fig. 5. Dependence of the spin-current polarization magnitude calculated at $z = 35$ nm on the bias voltage.

IV. CONCLUSION

We have presented a paradigm for electron spin transport in a GaMnAs/GaAs/GaMnAs heterostructure under external bias voltages. We have computed the spin-current profile for specified bias voltages and investigated the bias dependence of the two spin-current components responsible

for the field-like term and spin-transfer torque term in the LLGS equation governing the magnetization switching. The results provide a better understanding of the spin-current behavior and may help to shed light on the role of the spin current in the CIMS mechanism in semiconductor-based devices. For modeling real devices, the sum over all the in-plane waves and integration over energy needs to be taken. These procedures require a suitable parameter set to eliminate spurious states for all the in-plane wave-vector directions and refinement of the Landauer formula for spin current. This will be the aim of our future research.

ACKNOWLEDGMENT

Hoai T. L. Nguyen would like to acknowledge the International Center of Physics (Grant No. ICP. 2021.12) for support of this research. We are grateful to H. Jaffrès for valuable discussions.

REFERENCES

- [1] J. C. Slonczewski, *Current-driven excitation of magnetic multilayers*, *J. Magn. Magn. Mater.* **159** (1996) L1-L7.
- [2] L. Berger, *Emission of spin waves by a magnetic multilayer traversed by a current*, *Phys. Rev. B* **54** (13) (1996) 9353.
- [3] M. Elsen, O. Boulle, J. -M. George, H. Jaffrès, R. Mattana, V. Cros, A. Fert, A. Lemaitre, R. Giraud and G. Faini, *Spin transfer experiments on (Ga, Mn) As / (In, Ga) As / (Ga, Mn) As tunnel junctions*, *Phys. Rev. B* **73** (2006) 035303.
- [4] I. M. Miron, G. Gaudin, S. Auffret, B. Rodmacq, A. Schuhl, S. Pizzini, J. Vogel and P. Gambardella, *Current-driven spin torque induced by the Rashba effect in a ferromagnetic metal layer*, *Nat. Mater.* **9** (2010) 230.
- [5] Y. Wang, D. Zhu, Y. Wu, Y. Yang, J. Yu, R. Ramaswamy, R. Mishra, S. Shi, M. Elyasi, K. -L. Teo, Y. Wu and H. Yang, *Room temperature magnetization switching in topological insulator-ferromagnet heterostructures by spin-orbit torques*, *Nat. Commun.* **8** (2017) 1364.
- [6] M. Jiang, H. Asahara, S. Sato, T. Kanaki, H. Yamasaki, S. Ohya and M. Tanaka, *Efficient full spin-orbit torque switching in a single layer of a perpendicularly magnetized single-crystalline ferromagnet*, *Nat. Commun.* **10** (2019) 2590.
- [7] A. Manchon, J. Železny, I. M. Miron, T. Jungwirth, J. Sinova, A. Thiaville, K. Garello and P. Gambardella, *Current-induced spin-orbit torques in ferromagnetic and antiferromagnetic systems*, *Rev. Mod. Phys.* **91** (2019) 035004.
- [8] S. Bhatti, R. Sbiaa, A. Hirohata, H. Ohno, S. Fukami and S. N. Piramanayagam, *Spintronics based random access memory: a review*, *Mater. Today* **20**(9) (2017) 530.
- [9] E. I. Rashba, *Spin currents in thermodynamic equilibrium: The challenge of discerning transport currents*, *Phys. Rev. B* **68** (2003) 241315(R).
- [10] H. -J. Drouhin, G. Fishman and J. E. Wegrowe, *Spin currents in semiconductors: Redefinition and counterexample*, *Phys. Rev. B* **83** (2011) 113307.
- [11] P. M. Haney and M. D. Stiles, *Current-induced torques in the presence of spin-orbit coupling*, *Phys. Rev. Lett.* **105** (2010) 126602.
- [12] W. Cao, M. Wei-Yuan Tu, J. Xiao and W. Yao, *Giant spin transfer torque in atomically thin magnetic bilayers*, *Chinese Physics Letters* **37**(10) (2020) 107210.
- [13] N. S. Al-Shameri and H. Dakhlaoui, *Spin-current oscillations in diluted magnetic semiconductor multibarrier GaMnAs/GaAs: Role of temperature and bias voltage*, *Coatings* **12**(4) (2022) 504.
- [14] N. S. Al-Shameri and H. Dakhlaoui, *Numerical investigation of quantum tunneling time and spin-current density in GaAs/GaMnAs/GaAs barriers: Role of an applied bias voltage*, *Physica B* **628** (2022) 413555.
- [15] M. Tanaka, S. Ohya and Pham Nam Hai, *Recent progress in III-V based ferromagnetic semiconductors: Band structure, Fermi level, and tunneling transport*, *App. Phys. Rev.* **1** (2014) 011102.

- [16] D. To, T. Dang, Hoai Nguyen, V. Safarov, J. George, H. -J. Drouhin and H. Jaffrès, *Spin-orbit currents, spin-transfer torque and anomalous tunneling in III–V heterostructures probed by advanced 30- and 40-bands $k \bullet p$ tunneling methods*, *IEEE Trans. Magn.* **55**(7) (2019) 1400707.
- [17] Duy-Quang To, *Advanced multi-band $k.p$ methods for semiconductor-based spintronics*, Ph.D dissertation, Institut Polytechnique de Paris (2019).
- [18] Guy Fishman, *Semi-conducteurs: les bases de la théorie $k.p$* , Les Édition de l'École Polytechnique (2010).
- [19] S. Richard, F. Aniel and G. Fishman, *Energy-band structure of Ge, Si, and GaAs: A thirty-band $k \bullet p$ method*, *Phys. Rev. B* **70** (2004) 235204.
- [20] T. L. Hoai Nguyen, H. -J. Drouhin, and G. Fishman, *Spin trajectory along an evanescent loop in zinc-blende semiconductors*, *Phys. Rev. B* **80** (2009) 075207.
- [21] Y. Ando and T. Ito, *Calculation of transmission tunneling current across arbitrary potential barriers*, *J. Appl. Phys.* **61** (1987) 1497.
- [22] Nguyen Thi Loan and Nguyen Thi Lam Hoai, *Hong Duc University Journal of Science*, **45** (2019) 95.
- [23] A. Kalitsov, *Spin-polarized current-induced torque in magnetic tunnel junctions*, *J. Appl. Phys.* **99**(8) (2006) 08G501.
- [24] D. C. Ralph and M. D. Stiles, *Spin transfer torques*, *J. Magn. Magn. Mater.* **320** (2008) 1190.